IMPROVING SUPERSONIC FLOW AROUND BODIES BY MEANS OF GAS JETS CONTAINING PARTICLES

N. P. Gridnev

UDC 532.529

Particle-bearing gas jets provide a way of adjusting aircraft characteristics and reducing surface heat fluxes [1]. The physical principle resembles that for installing a sharp point at the leading edge of an aerodynamic model [2] in that one adjusts the flow structure near the body. Here is considered flow characteristics for bodies of rotation (cone joined to a cylinder or cylinder) arising in supersonic flow in the presence of a gas jet containing particles. The complete Navier–Stokes equations for a viscous conducting gas are solved by means of a third-order difference scheme [3, 4].

The cylinder and the cone attached to it are placed at zero angle of attack in the supersonic air stream: a two-dimensional formulation can be used. The jet emerges along the symmetry axis and its transverse dimension was less by a factor of 12 than that of the cylinder. It was assumed that the speed of the particles in the jet was equal to the speed of the jet at the exit hole, after which it decreased in a set fashion and became much less than the initial value at a certain distance from the body. At that instant, the leading particle is considered to halt. The mode of flow at that point is of interest. The halted particle is then entrained by the incident flow and carried downstream, with the leading particle replaced by a fresh one, with the flow pattern remaining the same in spite of a certain nonstationarity. The working grid has finite dimensions, so it is not possible to maintain a set relation between the sizes of the body and the particle, and therefore the diameter of the particles was taken as less than that of the body by a factor 12. In fact, the difference may be much greater. The distance at which a particle loses its velocity is dependent on the dynamic heads presented by the incident flow and the jet as well as on the particle's kinetic energy and shape. If necessary, it can be determined by experiment.

The Navier–Stokes equations were taken as

$$\frac{\partial \mathbf{f}}{\partial t} + \frac{\partial \mathbf{F}}{\partial x} + \frac{\partial \mathbf{G}}{\partial r} + \mathbf{\Phi} = 0,$$

$$\mathbf{f} = \begin{vmatrix} \rho \\ \rho u \\ \rho v \\ E \end{vmatrix}, \quad \mathbf{F} = \begin{vmatrix} \rho u \\ \rho u^2 - \sigma_x \\ \rho uv - \tau_{xr} \\ (E - \sigma_x) u - \tau_{xr} v - \lambda \dfrac{\partial T}{\partial x} \end{vmatrix}, \quad \mathbf{G} = \begin{vmatrix} \rho v \\ \rho uv - \tau_{xr} \\ \rho v^2 - \sigma_r \\ (E - \sigma_r) v - \tau_{xr} u - \lambda \dfrac{\partial T}{\partial r} \end{vmatrix},$$

$$\mathbf{\Phi} = \frac{1}{r} \begin{vmatrix} \rho v \\ \rho uv - \mu \dfrac{\partial u}{\partial r} + \dfrac{2}{3} \dfrac{\partial (\mu v)}{\partial x} - \mu \dfrac{\partial v}{\partial x} \\ \rho v^2 - 2\left[\mu \dfrac{\partial}{\partial r}\left(\dfrac{v}{r}\right) - \dfrac{1}{3} \dfrac{\partial}{\partial r}\left(\dfrac{\mu v}{r}\right)\right] \\ (E + p) v + \dfrac{4}{3} \mu \left[v \dfrac{\partial u}{\partial x} + rv \dfrac{\partial}{\partial r}\left(\dfrac{v}{r}\right)\right] \end{vmatrix},$$

$$E = c_V \rho T + \rho u^2/2 + \rho v^2/2, \quad \sigma_x = -p - \frac{2}{3} \mu \left(\frac{\partial u}{\partial x} + \frac{\partial v}{\partial r}\right) + 2\mu \frac{\partial u}{\partial x},$$

$$\sigma_r = -p - \frac{2}{3} \mu \left(\frac{\partial u}{\partial x} + \frac{\partial v}{\partial r}\right) + 2\mu \frac{\partial v}{\partial r}, \quad \tau_{xr} = \mu \left(\frac{\partial u}{\partial r} + \frac{\partial v}{\partial x}\right).$$

Novosibirsk. Translated from Zhurnal Prikladnoi Mekhaniki i Tekhnicheskoi Fiziki, No. 4, pp. 47-50, July-August, 1991. Original article submitted October 27, 1989.

0021-8944/91/3204-0508$12.50

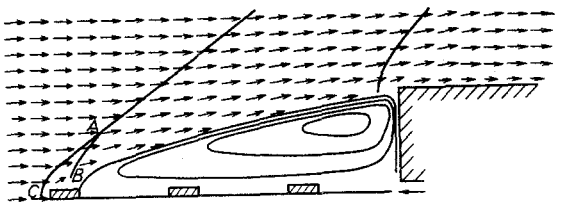

Fig. 1

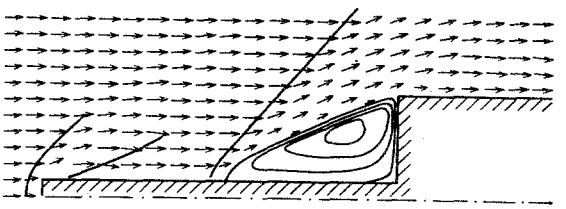

Fig. 2

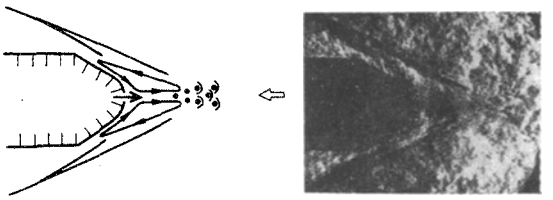

Fig. 3

The boundary conditions were specified as follows. At the symmetry axis, $\partial u/\partial r = \partial \rho/\partial r = \partial p/\partial r = v = 0$, while at the left-hand boundary in the working region, one has the parameters of the unperturbed incident supersonic flow. The flow parameters at the right-hand and upper boundaries are calculated for fictitious layers surrounding the working region from a first-order scheme from one-sided differences. It was also assumed that the surfaces of the body and particle are thermally insulated $(\partial T/\partial n = 0)$, while the attachment condition u = v = 0 applies there. The fictitious layers surrounding the body and particles from within have the values of the gas parameters determined from the conditions for compatibility between the boundary conditions and the equations.

At the start, the body is suddenly inserted into the uniform supersonic flow with the above boundary conditions. When the flow pattern is established, gas containing particles begins to flow from the central hole, with the particles following one another at distances of 0.6 of the body diameter. The calculation is terminated when the leading particle has attained its limiting distance ℓ (preset or derived from experiment). The calculations were performed with Prandtl number Pr = 0.7, specific-heat ratio $\gamma = 1.4$, and the assumption that the dynamic viscosity and thermal conductivity had a power-law dependence on temperature: $\mu = \mu_0(T/T_0)^{3/4}$, $\lambda = \lambda_0(T/T_0)^{3/4}$.

Figure 1 shows the flow pattern around the end of a cylinder with $M_\infty = 2$ and $Re_\infty = 1.36 \cdot 10^6$ (the cylinder diameter is taken as characteristic dimension). Jet parameters $\rho_c/\rho_\infty = 1$, $p_c/p_\infty = 4$, $u_c/a_\infty = 2$. The particles moving in the wake from the leader have subsonic velocities with respect to the surrounding gas and do not have any decisive effect on the mode of flow, the purpose being to replace the leader particle. Figure 2 shows the flow structure arising in flow around a cylinder with a point (with the same incident parameters) when the start of the point coincides with the tip of the leader particle. The differences between these flows lie only in the shape and extent of the detachment zone adjoining the head of the body.

If the particles are small and are distributed over the jet, there will be several leading particles. Then the shock-wave segment AC in Fig. 1 is replaced by a series of oblique shock waves that convert the incident supersonic flow to a subsonic one, while part AB vanishes. Figure 3 shows a scheme for the flow near the head of the model NV-1 together with the Töpler pattern. The change in flow pattern near the body in turn has substantial effects on the aerodynamic characteristics.

Figure 4 shows the radial pressure distribution at the end of the cylinder with various methods of influencing the flow. Curve 1 is the calculated distribution in the absence of any action, while the points are from experiment [5]. Curve 3 shows a point at the end of the cylinder, which corresponds to the [2] experiment with $Re_\infty/M = 1.36 \cdot 10^7$ and $\ell/R = 3.6$, in which ℓ is the length of the point and R the cylinder radius. Here the fit to experiment is determined from the resistance C_x. Curve 2 is the pressure distribution at the end of the cylinder when a gas jet free from particles emerges along the axis, which has parameters

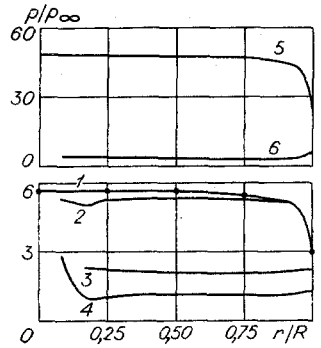

Fig. 4

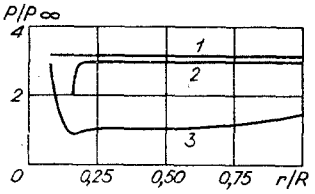

Fig. 5

$\rho_c/\rho_\infty = 1$, $p_c/p_\infty = 4$, $u_c/a_\infty = 2$. There is a slight reduction in the pressure at the end of the cylinder by comparison with the case of no action. Particles added to the jet reduce the frontal resistance considerably (curve 4). The jet energy is only 1% of the energy in the flow incident over the entire end area.

As the incident speed increases, so does the performance from the jet (by analogy with the use of a needle), as the upper part of Fig. 4 confirms from the calculated pressure distribution at the end for $M_\infty = 6$. Jet parameters $\rho_c/\rho_\infty = 1$, $p_c/p_\infty = 4$, $u_c/a_\infty = 6$. Curve 5 is for no action, while curve 6 is for a gas jet containing particles placed as for $M_\infty = 2$ in Fig. 1.

Figure 5 shows the pressure distribution on the cone with the cylinder, cone semivertex angle 30°. Curve 1 is for no action, $M_\infty = 2$ and $Re_\infty = 1.36 \cdot 10^6$. The aerodynamic characteristics are altered only slightly when a needle is installed with $\ell/R = 3.6$ (curve 2). A difference from the cylinder with needle (Fig. 4) is that no detachment zone arises with this net, since the pressure difference on the cone is slight. Although it is possible to detect a small detachment zone at the transition from the needle to the cone if the pitch is reduced considerably, it has no appreciable effect on the flow in the entire region. A jet containing particles emerging from the tip of the cone has an effect on the aerodynamic resistance more substantial than that from a needle (curve 3). Curves 4 and 6 in Fig. 4 and curve 3 in Fig. 5 have been obtained for the case of three leader particles. The basis for this is provided by a series of calculations and experiments that showed that it is best to have a jet containing several radially distributed leading particles, as in Fig. 3, particularly for flow around sharpened bodies. As the treatment is two-dimensional, the particles were represented as hoops with transverse sections of one working cell and were placed correspondingly at r = 0, R/4, and R/2.

As when a needle is used, a jet containing particles (mode 6 in Fig. 4) reduces the stagnation temperature at the end of the cylinder by comparison with mode 5 by a factor 1.5, which is important for high-speed supersonic flight, when it is necessary to reduce the heat fluxes to the walls of the vehicle, and when it becomes technically impossible to use a needle.

S. S. Katsnel'son suggested in 1980 that one should examine how a jet containing particles can influence incident supersonic flow in order to adjust aerodynamic characteristics. The experimental studies on this have been conducted under the guidance of V. P. Fomichev at the same institute (Institute of Theoretical and Applied Mechanics), who kindly provided his archive of Töpler patterns for the head of the NV-1 model shown in Fig. 3.

LITERATURE CITED

1. N. P. Gridnev, "Flow structure in viscous interaction between a shock wave and a moving particle," Zh. Prikl. Mekh. Tekh. Fiz., No. 2 (1987).
2. P. Chen, Flow Detachment Control [Rusian translation], Mir, Moscow (1979).
3. N. P. Gridnev, "A third-order difference scheme for calculating complicated gas-dynamic and magnetohydrodynamic flows," In: Aspects of Magnetic Gas Dynamics [in Russian], Inst-Theor. Prikl. Mekh. Sib. Otd. Akad. Nauk SSSR, Novosibirsk (1979).

4. N. P. Gridnev, S. S. Katsnel'son, and V. P. Fomichev, Inhomogeneous MHD Flows Containing T Layers [in Russian], Nauka, Novosibirsk (1984).
5. N. F. Krasnov, V. N. Koshevoi, A. N. Danilov, and V. F. Zakharchenko, Rocket Aerodynamics [in Russian], Vysshaya Shkola, Moscow (1968).